ENGINEERING TRANSACTIONS • *Engng. Trans.* • 40, 2, 159–176, 1992
Polish Academy of Sciences • Institute of Fundamental Technological Research

ESTIMATION OF THE FATIGUE LIFE OF THE FRONT AXLE OF A TRUCK

L. PROCHOWSKI (WARSZAWA)

Problems of dynamical loads and statistical characteristics of stresses in the front axle of a truck were considered. The probability of fatigue damages and the estimation of the fatigue life for various conditions of the vehicle's operation were calculated.

1. Introduction

The loads acting on the elements linking the body of a truck with the wheels are a consequence of, above all, the forces of action of the road on the wheels. Figure 1 shows that two types of loads can be distinguished, namely

the loads produced by intense breaking or lateral forces due to skidding or, finally, by occasional bumps of considerable height (at the crossing of a railway track, for instance) [1, 3] and

the loads resulting from the kinematic action of the unevenness of the road.

The results of the action of the loads classed (in a conventional manner) in the first or the second group can be taken into account during the computation of quasi-static or high-cycle fatigue strengths [2, 3, 5, 11], respectively.

Our attention will be focussed, however, on the loads due to the action of the roughness of the road on the wheels. The aim of the present paper is to analyse the characteristics of those loads with a view to estimate the fatigue life of the front axle of the truck.

2. Dynamic loads of the front axle

Let us consider the loads acting on the load-carrying system of a vehicle in steady rectilinear motion. Figure 1 shows the principal parameters used in the analysis of the load acting on the front axle F_T.

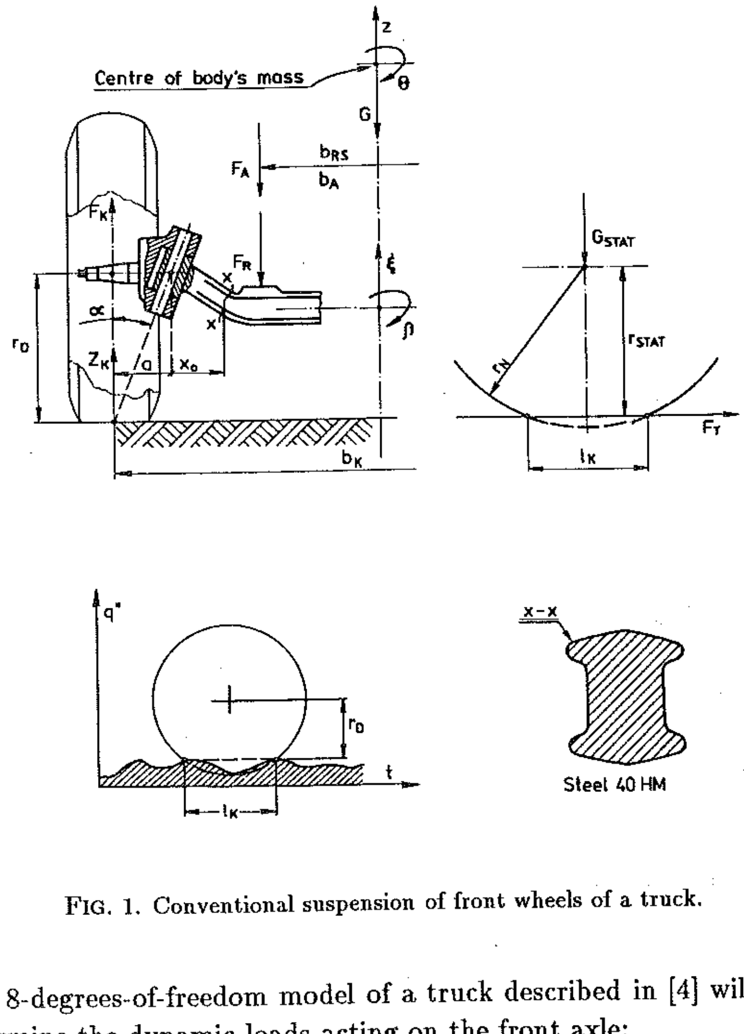

FIG. 1. Conventional suspension of front wheels of a truck.

The 8-degrees-of-freedom model of a truck described in [4] will be used to determine the dynamic loads acting on the front axle:

$$\begin{gathered} Z_K(t) = Z_{K,\mathrm{STAT}} + F_K(t) = Z_{K,\mathrm{STAT}} + c_K\left[r_{\mathrm{STAT}} - r_D(t)\right] - k_K \dot{r}_D(t)\,, \\ r_{\mathrm{STAT}} - r_D = y_K = q - \xi - 0.5\beta b_K\,, \quad |Z_{K,\mathrm{STAT}}| = |G_{\mathrm{STAT}}|\,, \end{gathered} \tag{2.1}$$

$$q(t) = \frac{v}{l_K} \int\limits_{t-\frac{l_K}{2V}}^{t+\frac{l_K}{2V}} q^*(\tau)\,d\tau\,, \tag{2.2}$$

where v is the travelling speed of the truck, $y_K(t)$ – dynamic deflection of the tyre, c_K, k_K – coefficient of radial stiffness and damping of the tyre, respectively, $q^*(t)$ – unevenness profile of the road, STAT – static equilibrium index.

The excitation acting on the left- and right-hand wheels of the model considered are different [6],

$$q_{Li}(t) \neq q_{pi}(t), \qquad q_{L2}(t) = q_{L1}(t-\tau), \qquad \tau = \frac{L}{V},$$

and can be reduced to

$$q_{1i} = \frac{q_{Li} + q_{pi}}{2}, \qquad q_{2i} = \frac{q_{Li} - q_{pi}}{2}, \qquad i = 1, 2, \tag{2.3}$$

where $q_1 \in \{q_{11}, q_{12}\}$ is the excitation acting in a symmetrical manner on the left- and right-hand wheels (producing vibration in the vertical plane), and $q_2 \in \{q_{21}, q_{22}\}$ – asymmetrical excitation (producing, above all, lateral angular vibrations), L – axle base, i – axle number.

Symmetrical and asymmetrical action of the road on the wheels are considered, the actions normal to the wheel plane due, for instance, to the transverse slope of an unevenness of the road being disregarded. The problem of such loads will be studied in a separate paper. Following many works ([6, 10, 13] and others) it will be assumed that the action $q(t)$ is stationary and of Gaussian distribution. The statistical characteristics of the excitation forces have been determined from the results of measurements of road roughness, which are presented in [7]. Under such conditions the statistical characteristics of the loads which will be used in what follows have a sense of estimators, the accuracy of which is directly connected with that of estimation of the spectral densities of excitation [6,7].

The equations of state of the model vehicle, which are presented in an explicit form in [4], can be expressed in the matrix form:

$$\mathbf{A}\ddot{\mathbf{u}} + \mathbf{B}\dot{\mathbf{u}} + \mathbf{C}\mathbf{u} = \mathbf{Q}, \tag{2.4}$$

where $\mathbf{u}$ is the vector of generalized coordinates, $\mathbf{u} \in \{\xi_1, \xi_2, \beta_1, \beta_2, \ldots\}$, and $\mathbf{Q}$ – the vector of excitation, $\mathbf{Q} \in \{q_{11}, q_{12}, q_{21}, q_{22}, 0, 0, 0, 0\}$.

By solving the equations of state we can determine the spectral transmittances of state variables and, on this basis, the spectral densities of the response of the model. Taking into account the structure of the excitations q_1 and q_2, three cases can be considered [4, 13]

1) $q_1 \neq 0, \quad q_2 = 0$. Then

$$
(2.5)\quad
\begin{aligned}
F_K^{(1)}(t) &= c_{K1}\,[q_{11}(t) - \xi_1(t)] + k_{K1}\left[\dot{q}_{11}(t) - \dot{\xi}_1(t)\right],\\
G_{FK}^{(1)}(\omega) &= G_{q_{11}}(\omega)\Big\{|\Phi_{11}^{FK}(j\omega)|^2 + \Phi_{11}^{FK}(j\omega)\,\overset{*}{\Phi}{}_{12}^{FK}(j\omega)e^{-j\omega\frac{L}{V}}\\
&\quad + \Phi_{12}^{FK}(j\omega)\,\overset{*}{\Phi}{}_{11}^{FK}(j\omega)e^{j\omega\frac{L}{V}} + |\Phi_{12}^{FK}(j\omega)|^2\Big\}\\
&= G_{q_{11}}(\omega)|\Phi_1^{FK}(j\omega)|^2,
\end{aligned}
$$

where $G_{FK}^{(1)}$ is the spectral density of dynamic loads $F_K^{(1)}$, $G_{q_{11}}$ – spectral density of the excitation q_{11}, $\Phi_{11}^{FK}(j\omega) = \frac{F_K(j\omega)}{q_{11}(j\omega)}$ – spectral transmittance expressing the ratio of the Laplace transform of the variable $F_K(t)$ to the excitation transform $q_{11}(t)$, and $*$ is an index denoting a conjugate complex variable, $\omega = 2\pi f$, where f is the frequency and $j = \sqrt{-1}$.

2) $q_1 = 0, \quad q_2 \neq 0$. Then

$$
(2.6)\quad
\begin{aligned}
F_K^{(2)}(t) &= c_{K1}\left[q_{21}(t) - \beta_1(t)\frac{b_{K1}}{2}\right] + k_{K1}\left[\dot{q}_{21}(t) - \dot{\beta}_1(t)\frac{b_{K1}}{2}\right],\\
G_{FK}^{(2)}(\omega) &= G_{q_{21}}(\omega)\Big\{|\Phi_{21}^{FK}(j\omega)|^2 + \Phi_{21}^{FK}(j\omega)\,\overset{*}{\Phi}{}_{22}^{FK}(j\omega)e^{-j\omega\frac{L}{V}}\\
&\quad + \Phi_{22}^{FK}(j\omega)\,\overset{*}{\Phi}{}_{21}^{FK}(j\omega)e^{j\omega\frac{L}{V}} + |\Phi_{22}^{FK}(j\omega)|^2\Big\}\\
&= G_{q_{21}}(\omega)|\Phi_2^{FK}(j\omega)|^2;
\end{aligned}
$$

3) $q_1 \neq 0, \quad q_2 \neq 0$. Then

$$
(2.7)\quad
\begin{aligned}
G_{FK}(\omega) &= |\Phi_1^{FK}(j\omega)|^2 G_{q_{11}}(\omega) + \Phi_1^{FK}(j\omega)\,\overset{*}{\Phi}{}_2^{FK}(j\omega)G_{q_{11}q_{21}}(j\omega)\\
&\quad + \Phi_2^{FK}(j\omega)\,\overset{*}{\Phi}{}_1^{FK}(j\omega)G_{q_{21}q_{11}}(j\omega) + |\Phi_2^{FK}(j\omega)|^2 G_{q_{21}}(\omega),
\end{aligned}
$$

where $G_{q_{11}q_{21}}$ is the cross-spectral density of the functions $q_{11}(t)$ and $q_{21}(t)$.

Figure 2 shows the amplitude-frequency characteristics of the principal load components acting on the front axle,

$$
(2.8)\quad
\begin{aligned}
A_{FK}(\omega) &= |\Phi^{FK}(j\omega)|, && F_K \text{ is the force in the wheel axle,}\\
A_{FA}(\omega) &= |\Phi^{FA}(j\omega)|, && F_A \text{ is the force in the shock absorber,}\\
A_{FR}(\omega) &= |\Phi^{FR}(j\omega)|, && F_R \text{ is the force in the leaf spring.}
\end{aligned}
$$

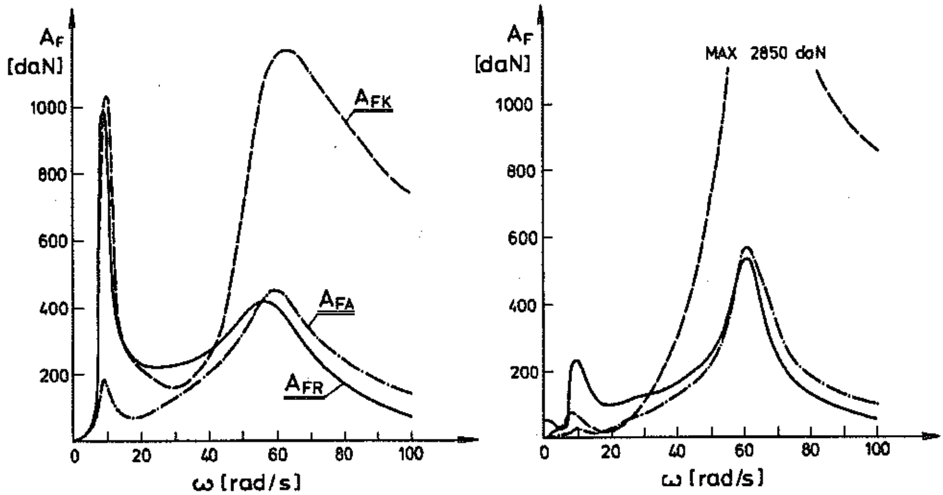

FIG. 2. Amplitude-frequency characteristics of the load on the front axle; symmetrical and asymmetrical excitation.

The type of variation of those quantities means that the proportion of high-frequency components in the loads acting on the wheels is considerable. The diagrams in Fig.3 illustrate what is termed partial systems [9], which

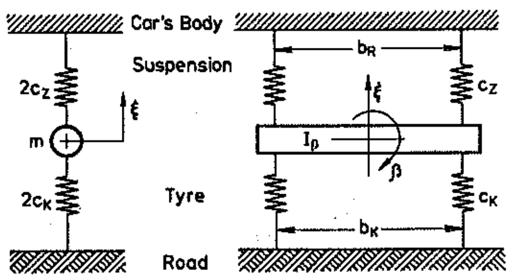

FIG. 3. Diagrammatic representation of system used for computing natural frequencies.

are often made use of for computing natural vibrations of the front axle beam:

$$\omega_\xi = \sqrt{\frac{2c_Z + 2c_K}{m}} \qquad \omega_\beta = \sqrt{\frac{b_R^2 c_Z + b_K^2 c_K}{2I_\beta}}\,. \tag{2.9}$$

In the model truck considered, the fundamental characteristics of which approach those of the STAR 1142 truck, the theoretical natural frequencies are

$$\omega_\xi \cong 58\,\tfrac{\text{rad}}{\text{s}}, \qquad f_\xi \cong 9.2\,\text{Hz},$$
$$\omega_\beta \cong 61\,\tfrac{\text{rad}}{\text{s}}, \qquad f_\beta \cong 9.7\,\text{Hz},$$

The importance of the dominant modes which correspond to those frequencies and which can be seen on the amplitude-frequency characteristics is confirmed by the results of the tests presented, among other papers, in [8]. On the other hand, the dominating amplitudes of the operational loads on the front axle (Fig.4) depend on the vibrations of both the body of the truck and the axles of the wheels. The contribution of the two excitation components (q_1, q_2) to the generation of the loads acting on the wheel axles are comparable.

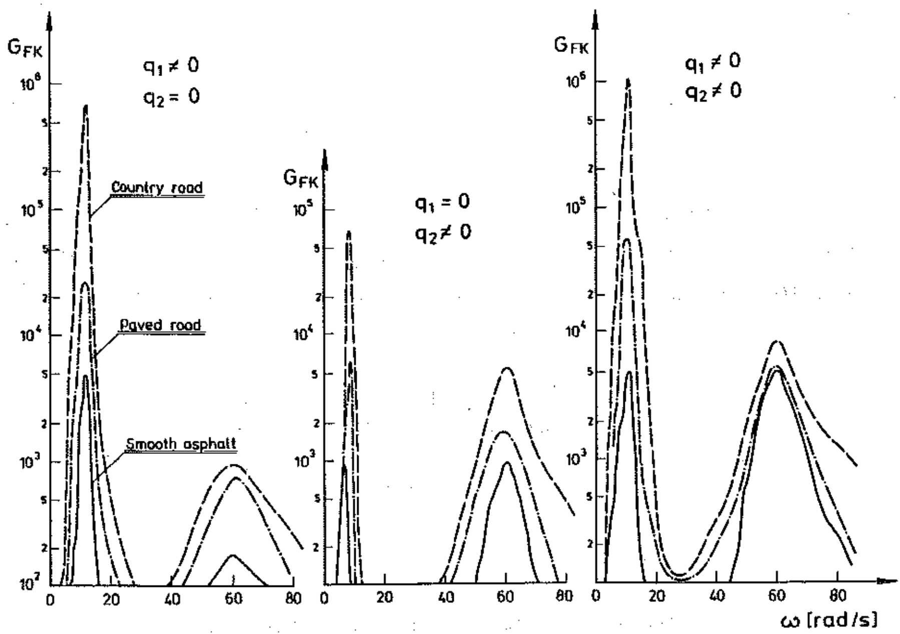

FIG. 4. Estimators of spectral densities of loads acting of the wheel axles $V = 40$ km/h.

The spectral densities (2.5), (2.6) and (2.7) having been determined, we can determine the variance of the load F_K and those of its first and second derivative, that is

$$\delta_{FK}^2 = \int_0^{\omega_{\max}} G_{FK}(\omega)\, d\omega, \tag{2.10}$$

(2.10) [cont.]
$$\delta^2_{\dot{F}K} = \int_0^{\omega_{\max}} \omega^2 G_{FK}(\omega)\, d\omega\,,$$
$$\delta^2_{\ddot{F}K} = \int_0^{\omega_{\max}} \omega^4 G_{FK}(\omega)\, d\omega\,.$$

δ_{FK} – standard deviation of F_K

This results has been used to calculate following indices of dynamic load on the wheel axles, that is

the coefficient of width of the frequency band of the load

$$I_S = \frac{\delta^2_{\dot{F}K}}{\delta_{FK}\delta_{\ddot{F}K}}\,; \tag{2.11}$$

the mean number of peaks per 1 km of the road and their mean frequency of occurrence

$$a_M = \frac{3600}{2\pi v}\frac{\delta_{\ddot{F}K}}{\delta_{\dot{F}K}}\,, \qquad \text{V[km/h]}\,,$$
$$f_M = \frac{a_M V}{3600}\,.$$

Table 1 contains the values characterizing the state of load on the wheel axles for two models of the truck (with full load).

model 1 $\quad Z_{K,\mathrm{STAT}} = 2000$ daN,

model 2 $\quad Z_{K,\mathrm{STAT}} = 4000$ daN.

In the Model 2, for which the static load acting on the wheel axles is twice as high as that for the Model 1, the characteristics of the suspension and the tyres have been changed to suit the required load carrying capacity of the system.

The dynamic loads on the wheel axles increase with increasing velocity of motion and increasing height of the irregularities of the surface. It is worthwhile to observe that $\delta_{FK} > 0.5Z_{K,\mathrm{STAT}}$ for $V = 40$ km/h for soil-surfaced road. Such a high degree of dynamic load is frequently a cause of contact loss between the wheels and the road, which impairs considerably the travel safety. Dynamic loads due to the motion of the vehicle on soil-surfaced and paved roads are of the wide-band type $I_s < 0.7$. The mean number of peaks and the frequency of their occurrence depend little on the road conditions. A decisive influence on those quantities is that of the natural frequencies of the road wheel axles and the coupling between the

Table 1. Characteristics of dynamic loads for $q_1 \neq 0$, $q_2 \neq 0$.

$Z_{K,\mathrm{STAT}}$	δ_y, δ_{q1} – standard deviation (estimators) of the deflection of the tyre and the unevenness of the road, $V = 20$ km/h														
	asphalt, $\delta_{q1} = 0.64$ cm					paved, $\delta_{q1} = 1.29$ cm					country road, $\delta_{q1} = 4.30$ cm				
[daN]	δ_{FK}	δ_Y	a_M	f_M	I_s	δ_{FK}	δ_y	a_M	f_M	I_s	δ_{FK}	δ_y	a_M	f_M	I_s
	daN	cm	$\frac{1}{\mathrm{km}}$	$\frac{1}{\mathrm{s}}$	–	daN	cm	$\frac{1}{\mathrm{km}}$	$\frac{1}{\mathrm{s}}$	–	daN	cm	$\frac{1}{\mathrm{km}}$	$\frac{1}{\mathrm{s}}$	–
2000 daN	70	0.12	1780	9.9	0.52	190	0.33	1670	9.3	0.38	280	0.50	1760	9.7	0.41
4000 daN	190	0.17	1750	9.7	0.37	540	0.48	1610	8.8	0.34	760	0.68	1660	9.2	0.31
	$v = 40$ km/h														
2000 daN	260	0.39	1070	11.9	0.77	470	0.75	1050	11.7	0.63	1430	2.50	1100	12.2	0.32
4000 daN	550	0.49	1100	12.2	0.65	1120	1.00	1090	12.1	0.45	4220	3.77	1000	11.1	0.25
	$v = 60$ km/h														
2000 daN	350	0.47	940	15.6	0.70	620	1.00	860	14.3	0.60	$\delta_{FK} \gg Z_{K,\mathrm{STAT}}$				
4000 daN	800	0.70	950	15.9	0.60	1470	1.30	890	14.9	0.45					

vibrations of the front and the rear part of the vehicle. With increasing V the frequency of occurrence of peaks f_M also increases, begining with values approaching f_ξ and f_β, for low V, and reaching much higher values; this is connected with increasing vibration of the front axle and also with the displacement of the local dominants of spectral density of excitation (with increasing V) towards higher values of the frequencies [4, 6, 8].

The values obtained for the standard deviations δ_{FK} approach those presented in the paper [12], which contains the results of measurement of the loads acting on the front axle of a wheeled tractor. For a static load approaching the Model 1 considered here, it was found that

$$\delta_{FK} = 164 - 184\,\mathrm{daN} \quad \text{for } V = 17 - 22\,\mathrm{km/h}\,, \quad \delta_{q_1} = 1.1\,\mathrm{cm}\,.$$

3. Loads spectrum of the front axle

As regards strength computation of the front axle of a truck, the most important cross-section lies, as a rule, in the neighbourhood of the mounting point of the leaf spring [1,3] (Fig.1). This is a region of possible damage, often occurring in the form of plastic deformation of the axle. The bending stress in the cross-section $x - x$ can be determined from the relation

$$\sigma_G \cong \frac{a + x_0}{W_x} Z_K\,, \qquad Z_K(t) = Z_{K,\mathrm{STAT}} + F_K(t)\,.$$

We have, of course,

$$\sigma_G(t) = \sigma_{G,\mathrm{STAT}} + \sigma_{G,\mathrm{DYN}}(t) \cong \frac{a + x_0}{W_x} Z_{K,\mathrm{STAT}} + \frac{a + x_0}{W_x} F_K(t)\,, \tag{3.1}$$

where

$$a(t) = [r_{\mathrm{STAT}} - y(t)]\,\mathrm{tg}\alpha = r_{\mathrm{STAT}}\mathrm{tg}\alpha - y(t)\mathrm{tg}\alpha\,,$$

$$a \cong r_{\mathrm{STAT}}\mathrm{tg}\alpha \quad \text{when} \quad y(t) \ll r_{\mathrm{STAT}}\,.$$

The results of analysis of the state of load on the front axle enable us to assume that $F_K(t)$ is stationary process with Gaussian distribution at

$$E[F_K(t)] \cong 0\,,$$

where E is the mean value operator.

Therefore

$$E[\sigma_{G,\mathrm{DYN}}(t)] \cong 0\,.$$

Then

$$E[\sigma_G(t)] = \sigma_M \cong \frac{a+x_0}{W_x} Z_{K,\mathrm{STAT}}$$

$$\delta_G \cong \frac{a+x_0}{W_x}\delta_{FK},$$

δ_G – standard deviation of the stress.

Using the observed values of I_s (index of width of the load spectrum), the variation of the mean values and the amplitudes of particular load cycles separated from $\sigma_{G,\mathrm{DYN}}(t)$ should be taken into account. The results of tests of dynamic loads on vehicles [11, 8] justify the assumption that the distribution of the mean values $\bar{\sigma}_M$ is a Gaussian distribution and that of load cycles σ_A – a Rayleigh distribution. Then, the probability density of peak values can be described by the Rice relation

$$p(\sigma) = \frac{\beta_\omega}{\sqrt{2\pi}\,\delta_\sigma} \exp \frac{\sigma^2}{2\beta_\omega^2\,\delta_\sigma^2} + \frac{\sigma\sqrt{1-\beta_\omega^2}}{\sqrt{2\pi}\,\delta_\sigma^2} \exp\left(-\frac{\sigma^2}{2\delta_\sigma^2}\right) \int\limits_{-\infty}^{\frac{\sqrt{1-\beta_\omega^2}}{\beta_\omega\delta_\sigma}\sigma} \exp\left(-\frac{\tau^2}{2}\right) d\tau, \tag{3.2}$$

where δ_σ is the standard deviation of the stress

$$\beta_\omega = \sqrt{1-I_S^2}\,. \tag{3.3}$$

The notion of amplitude used here has no complete physical interpretation (a wide-band process) and is connected with the assumption that each peak value of the process $\sigma(t)$ determines a load cycle between the consecutive maximum and minimum. Thus the k-th load cycle can be described by the mean value of the cycle $\bar{\sigma}_{Mk}$ and its amplitude σ_{Ak}.

Figure 5 shows the probability distribution of the amplitude of load (the stress in the cross-section $x-x$) due to the motion of the vehicle on an asphalt, paved and soil surface at a velocity $V = 40$km/h. The value of the static load $\sigma_M = \sigma_{\mathrm{STAT}}$ has been assumed as a reference level for the distributions of load amplitude just mentioned. The limiting values of the amplitude distribution were determined as follows:

$$\begin{aligned} \sigma_{\mathrm{MAX}} &= \sigma_{\mathrm{STAT}} + k_\sigma\delta_\sigma\,, \\ \sigma_{\mathrm{MIN}} &= \sigma_{\mathrm{STAT}} - k_\sigma\delta_\sigma\,, \end{aligned} \tag{3.4}$$

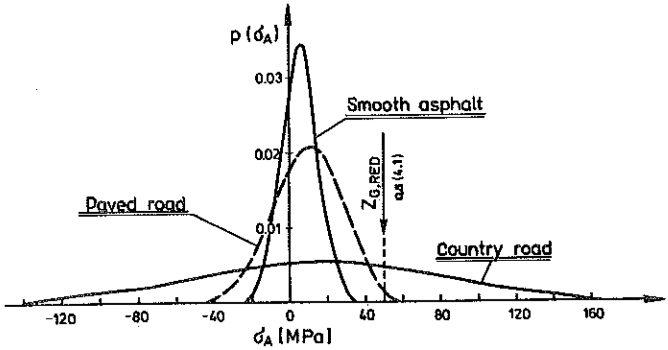

FIG. 5. Probability distribution of stress amplitudes (peak values) due to symmetrical action on the wheels, $V = 40$ km/h.

where k_σ is the limiting coefficient of the maximum value.

The loads, the probability $p(\sigma)$ of occurrence of which is below 10^{-5} are disregarded, therefore

$$\int_{\sigma_{\mathrm{MAX}}}^{infty} p(\sigma)\,d\sigma = 10^{-5}\,. \tag{3.5}$$

Hence $k_\sigma = 4.27$.

Table 2. Relation between the kind of the road surface and the state of dynamic loads on the vehicle (symmetric action on the wheels, $q_1 \neq 0$, $q_2 = 0$).

Road surface $V = 40$ km/h	δ_{q_1} [cm]	$\delta_{\ddot{z}}$ [cm/s^2]	cross-section $x - x$		
			δ_σ [MPa]	$p\,(\sigma_A > Z_{G,\mathrm{RED}})$	life estimate in km
asphalt	0.64	86	8.12	< 0.00001	> 10000000
paved	1.29	220	19.9	0.02	92000
country road	4.30	900	78.3	0.32	260

$Z_{G,\mathrm{RED}}$ – according to 4.1; $\sigma_{\ddot{z}}$ – standard deviation of the acceleration of the truck body.

Table 2 contains the values of standard deviations of the height of the irregularities of the road surfaces mentioned above as well as the quantities characterizing the dynamic loads acting on the vehicle. Those values show that the influence of the variation in height of the irregularities of the road surface on the dynamic loads acting on the vehicle system and its durability is essential.

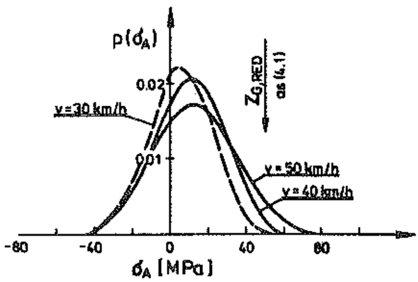

FIG. 6. The influence of the travelling speed on the distribution of $p(\sigma_A)$. Boulder paved road. Symmetrical action on the wheels.

Figure 6 illustrates the influence of a variation in the travelling speed on the stress amplitude distribution in the cross-section $x - x$ (Fig.1) of the front axle. With increasing V the diagram of probability distribution becomes more flat, thus showing an increase in probability of occurrence of cycles with amplitudes $\sigma_A > Z_G$ (fatigue limit). Load cycles with amplitudes above the fatigue limit Z_G are decisive for the life of the structural element analysed.

In agreement with (2.3) the model tests included the determination of dynamic loads due to symmetrical and asymmetrical forces acting on the vehicle wheels.

The relations between the results of the action of both excitation components (q_1, q_2) originating from the road are described in detail in [4]. Figure 7 shows the influence of the excitation components on the probability distribution of stress amplitudes. The effect of superposition of the results of action of both excitation components, which is natural for the vehicle and is described in the analytic manner in (2.7), is manifested by the increase in load amplitudes (dashed line in Fig.7). The values in Table 3 show that superpose of resonance dominants (cf. Fig.4) as a result of summation of the results of simultaneous action of the excitations q_1 and q_2 produces also the increase in load amplitudes and, consequently, an increase in the coefficient I_s. The common action of those two phenomena reduce the fatigue life of the structure.

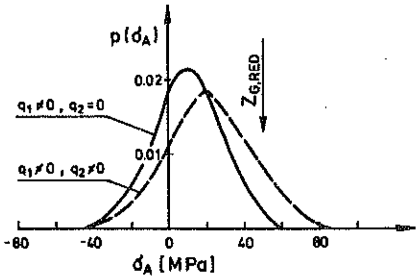

FIG. 7. The influence of the traveling speed on the distribution of $p(\sigma_A)$. Boulder paved road; $V = 40$km/h.

Table 3. The influence of the structure of excitations acting on the vehicle wheels on the state of load of the front axle in the cross-section $x - x$. Paved road; $V = 40$ km/h.

Excitation	$p(\sigma_A > Z_{G,\mathrm{RED}})$	I_s	Estimated life
$q_1 \neq 0$, $q_2 = 0$	0.02	0.41	92000 km
$q_1 \neq 0$, $q_2 \neq 0$	0.13	0.63	9600 km

4. Estimation of fatigue life

It is assumed that the Wöhler diagram of fatigue life of a structural element may be expressed by the relation [2]

$$\begin{aligned} \sigma_A^{m_1} N &= C \qquad \text{for} \qquad N \leq N_0 , \\ \sigma_A &= Z_G \qquad \qquad \quad N > N_0 . \end{aligned}$$

Knowing the probability distribution of load amplitude $p(\sigma_A)$, the life L_c of the element can be calculated in kilometers of mileage, on the basis of the Palmgren-Miner theory [2, 11] of cumulation of fatigue damages

$$L_C^{PM} = \frac{N_0}{a_M \int\limits_{Z_G}^{\sigma_{A,\mathrm{MAX}}} \left(\frac{\sigma_A}{Z_G}\right)^{m_1} p(\sigma_A)\, d\sigma_A}, \tag{4.1}$$

where $\sigma_{A,\mathrm{MAX}} = k_\sigma \delta_\sigma$, $Z_G \rightarrow Z_{G,\mathrm{RED}} = k_z(Z_G - \psi\sigma_M)$, k_z is influence coefficient of the stresses below the fatigue limit, ψ – coefficient of sensitivity of the material to asymmetry of load cycles.

In the practice of computation of fatigue life it is preferred to calculate simultaneously the mileage (the operation time) on the basis of several different theories of cumulation of fatigue damages. Under such conditions, making use of the relations given by Serensen and Haibach, it was also found that [2, 11]

$$
\begin{aligned}
L_C^{S_1} &= \frac{a_S N_0}{a_M \int\limits_{Z_G}^{\sigma_{A,\mathrm{MAX}}} \left(\frac{\sigma_A}{Z_G}\right)^{m_1} p(\sigma_A)\, d\sigma_A}, \\
(4.2)\; L_C^{S_2} &= \frac{a_R N_0}{\mathrm{a.m.}}, \\
L_C^{H} &= \frac{N_0}{a_M \left[\int\limits_{\sigma_{A,\mathrm{MIN}}}^{Z_G} \left(\frac{\sigma_A}{Z_G}\right)^{m_2} p(\sigma_A)\, d\sigma_A + \int\limits_{Z_G}^{\sigma_{A,\mathrm{MAX}}} \left(\frac{\sigma_A}{Z_G}\right)^{m_1} p(\sigma_A)\, d\sigma_A \right]};
\end{aligned}
$$

$$
(4.3)\quad a_R = \frac{\int\limits_{\sigma_{A,\mathrm{MIN}}}^{\sigma_{A,\mathrm{MAX}}} \sigma_A p(\sigma_A)\, d\sigma_A - \sigma_{A,\mathrm{MIN}} \int\limits_{\sigma_{A,\mathrm{MIN}}}^{\sigma_{A,\mathrm{MAX}}} p(\sigma_A)\, d\sigma_A}{\left(\sigma_{A,\mathrm{MIN}} - \sigma_{A,\mathrm{MAX}}\right) \int\limits_{\sigma_{A,\mathrm{MIN}}}^{\sigma_{A,\mathrm{MAX}}} p(\sigma_A)\, d\sigma_A},
$$

where $a_s = 0.1 \ldots 0.2$ is the Serensen coefficient, and m_1, m_2 are the coefficients of the slope of the left-hand and right-hand branch of Wöhler diagram, which is given, for computation of L_C^H, by the relation

$$
\begin{aligned}
\sigma_A^{m_1} N &= C_1 \quad \text{for} \quad N \le N_0, \\
\sigma_A^{m_2} N &= C_2 \quad \text{for} \quad N > N_0.
\end{aligned}
$$

Following [11] it was assumed that

$$
L_C^S = \begin{cases} L_C^{S_1} & \text{if} \quad a_R < a_S, \\ L_C^{S_2} & \text{if} \quad a_R \ge a_S. \end{cases}
$$

Experimental results show that an analysis based on the Palmgren-Miner or Haibach theory give results approaching the upper bound of the estimated value of the fatigue life of the element considered, while the Serensen theory leads to results approaching the lower bound of the fatigue life. Figure 8 compares the results of computation of the expected fatigue life in a manner showing the contribution of both the excitation components (q_1 for vertical vibrations and q_2 for horizontal angular vibrations) in the process of cumulation of fatigue damages.

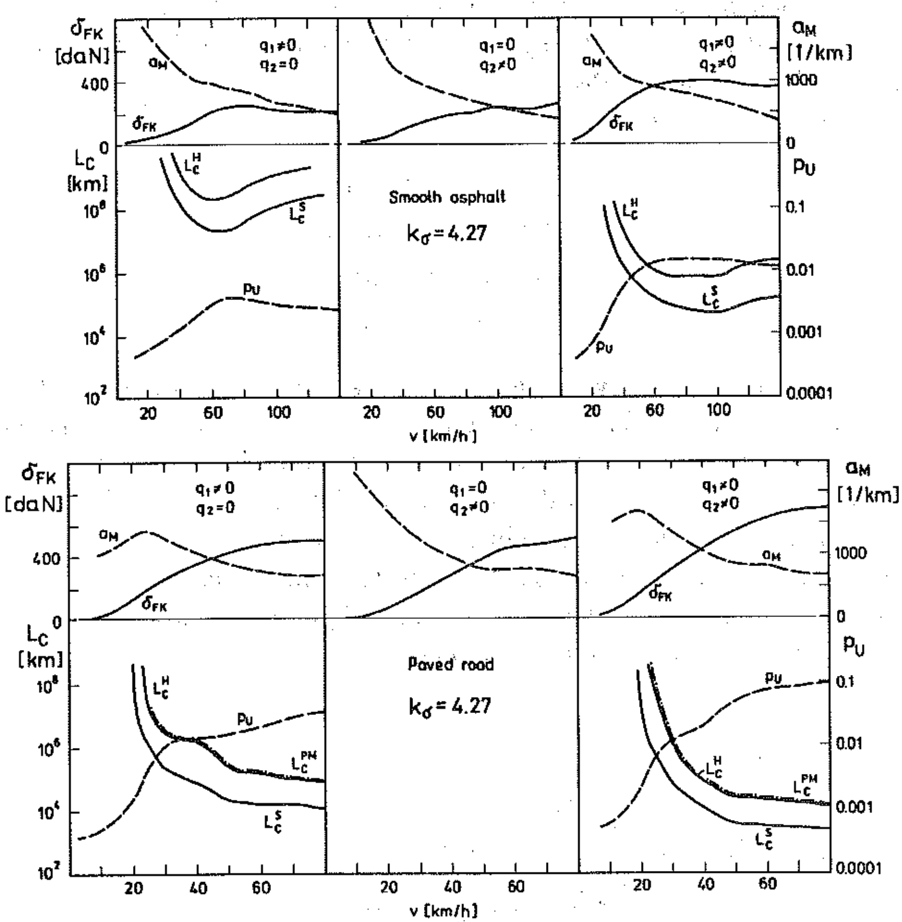

FIG. 8. Estimates of statistical characteristics of the loads and a forecast of the fatigue life of the front wheel axles.

Making use of the results of model studies available, the probability of plastic deformation (constituting the overloading damage) in the cross-section of the front axle considered was calculated. It was assumed for the analysis that the distribution of stress amplitude and that of yield limit are of the Gaussian type. Then, the probability of damage is

$$p_U = p(\sigma > R_E)\,,$$

where $\sigma(t)$ is the variation of the stress, its mean value being $\sigma_M = \sigma_{\mathrm{STAT}}$ and the standard deviation δ_σ . The symbols R_E and σ_{RE} denote the mean value and the standard deviation of the plasticity limit R_E of the structural element considered, respectively. The material assumed for computation was 40 HM ($R_E = 687$ MPa).

It was found for section $x - x$

$$\begin{aligned} R_E &= 172\,\mathrm{MPa}, \\ Z_G &= 107\,\mathrm{MPa}, \\ W_X &= 43\,\mathrm{cm}^3, \\ \sigma_{\mathrm{STAT}} &= 116\,\mathrm{MPa}. \end{aligned}$$

The results of the analysis presented in Fig.8 show that the character of variation of the fatigue life of the front axle as a function of the travelling speed of the truck may constitute, to a considerable degree, a reflection of the variation of the standard deviation of the forces in the wheel axle. We observe also an advantageous influence of the decrease in number of load cycles a_M (with increasing V) on the value L_C, thus enabling us to increase the mileage at high V. The reduction in fatigue life is closely connected with an increase in probability of damage.

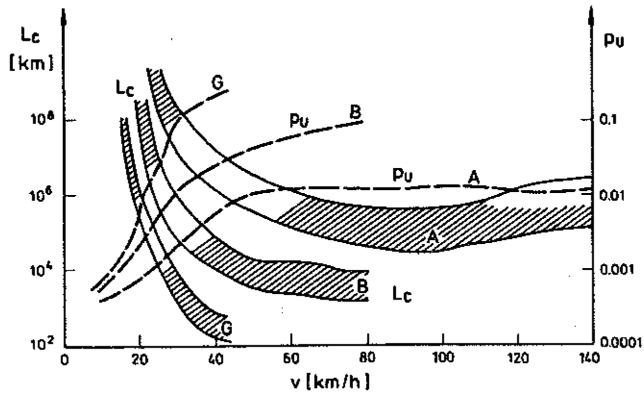

FIG. 9. Computation results of the fatigue life L_C and the probability of damage p_u for various travelling speeds. A – asphalt; B – boulder pavement; G – soil surface.

Figure 9 illustrates the variation of the estimated fatigue life L_C and the probability of damage p_U as function of the travelling speed of the truck. Confrontation of those variations shows the relations which may exist between the state of the pavement and the fatigue life of the front axle. High probability of damage of the front axle produces a necessity of reducing the travelling speed on a soil-surfaced or paved road.

5. Conclusions

The theoretical results presented here concern the range of limited fatigue life. Estimation of the fatigue life by the procedure presented is closely connected with the relation (3.1) and can be made use of as a criterion for improving the design of the vehicle. Another practical advantage of this theoretical forecast is that a relation is indicated between the excitations considered and the structure of the loads acting on the vehicle under various operating conditions, and the fatigue life of vehicle elements. This applies in particular to the mutual relations between the road surface and the travelling velocity as those operating factors which may be decisive for the resulting fatigue life of the vehicle.

References

1. K.Studziński, *The motor car: theory, design and computation* [in Polish], WKL, Warszawa 1980.
2. S.Kocańda and J.Szala, *Principles of fatigue analysis* [in Polish], PWN, Warszawa 1985.
3. J.Reimpell, *Fahrwerktechnik: Federung Fahrwerkmechanik*, Würzburg 1983.
4. L.Prochowski, *The structure of dynamic loads on a motor car moving on an asphalt road* [in Polish], Biul. WAT, 8, 1990.
5. **В.П.Жигарев, Л.Н.Куманьков, Г.Г.Сайдов, А.А.Хачатуров, Об источниках повышенных воздействий дороги на транспортные средства при движении по маршрутах большой протяженности, Труды МАДИ, Москва** 1983.
6. L.Prochowski, *Statistical estimates of the excitations acting on a vehicle moving on an asphalt road* [in Polish], Enging. Trans., **35**, 3, 1987.
7. L.Prochowski, *Statistical characteristics of excitations acting on a vehicle and originating from road* [in Polish], Enging. Trans., **38**, 2, 1990.
8. N.N.Jacenko, *Vibrations, strength and accelerated tests of trucks* [in Polish], WKL, Warszawa 1975.
9. J.Osiecki, *Modelling elements in dynamics of machines. A collection of papers on dynamics of machines* [in Polish], Ossolineum, 1974.
10. M.Mitschke, *Dynamics of a motor car* [in Polish], WKL, Warszawa 1977.

11. В.С.Лукинский, Ю.Г. Котиков, Е.И. Зайцев, Далговечность деталей шассы автомобиля, Машиностроение, Ленинград 1984.

12. А.П. Хилько, В.П. Бойков, С.И. Стигунов, Спектральный анализ нагруженности передней оси трактора МТЗ-80... ,Автотракторостроенние, 13, Минск 1979.

13. M.APETAUR, *Remarks on the theory of vehicle vibrational analysis based on the on-the-road measurements*, Vehicle System Dynamics, 11, 1982.

MILITARY TECHNICAL ACADEMY, WARSZAWA.

Received August 13, 1990; new version February 2, 1991.